# Energy management of a building cooling system with thermal storage: an approximate dynamic programming solution

R. Vignali[1], F. Borghesan[1], L. Piroddi[1], M. Strelec[2] and M. Prandini[1]

***Abstract*—The paper concerns the design of an energy management system for a building cooling system, that includes a chiller plant (with two or more chiller units), a thermal storage unit and a cooling load. The latter is modeled in a probabilistic framework to account for the uncertainty in the building occupancy. The energy management task essentially consists in the minimization of the energy consumption of the cooling system, while preserving comfort in the building. This is achieved by a two-fold strategy. The cooling power request is optimally distributed among the chillers and the thermal storage unit. At the same time, a slight modulation of the temperature set-point of the zone is allowed, trading energy saving for comfort. The problem can be decoupled into a static optimization problem (mainly addressing the chiller plant optimization) and a dynamic programming (DP) problem for a discrete time stochastic hybrid system (SHS), that takes care of the overall energy minimization. The DP problem is solved by abstracting the SHS to a (finite) controlled Markov chain, where costs associated to state transitions are computed by simulating the original model and determining the corresponding energy consumption. A numerical example shows the efficacy of the approach.**

***Note to Practitioners*—Heating and cooling systems for buildings present difficult energy management problems due to the interaction of complex devices, such as chillers and thermal storages, and the dependence on uncertain variables, such as building occupancy and external temperature. This paper addresses the minimization of the energy consumption in a building endowed with a cooling system and exploiting a thermal storage unit (essentially a tank storing cool water) to drive the cooling system more efficiently. A further degree of freedom is introduced in the optimization process, related to a limited relaxation of the user comfort request. The methodology explained in the paper is extendable to more complex micro-grids, including *e.g.* additional electric appliances, renewable energy sources or co-generation units.**

***Index Terms*—Approximate dynamic programming, cooling systems, energy management, stochastic hybrid systems, Markov chain abstraction.**

## I. Introduction

In this paper, we focus on the energy management of a building cooling system, consisting of a chiller plant, a small thermal storage unit, and a cooling load, as sketched in Fig. 1. The cooling load represents the cooling energy needed to maintain some temperature profile in a zone (which can be a room, several rooms or a partitioned space in a room) subject to two main sources of heating power, *i.e.* the outside ambient temperature and the internal heat gains due to the presence of people, office equipment, lighting, etc. The second heating source, synthetically attributed to people occupancy, is here described using a probabilistic model. The chiller plant is composed of $n$ chillers that convert into cooling power the electric power provided by the distribution grid through the Local Power Network (LPN). The cooling power is conveyed to the cooling load through the Chilled Water Circuit (CHWC). The chillers are generally characterized by different efficiency curves, their performance depending on the outside ambient temperature, the temperature of the cooling medium, and the requested cooling power [1]. The thermal storage unit can be used to accumulate cooling power and deliver it when needed, and, hence, add some flexibility to the system.

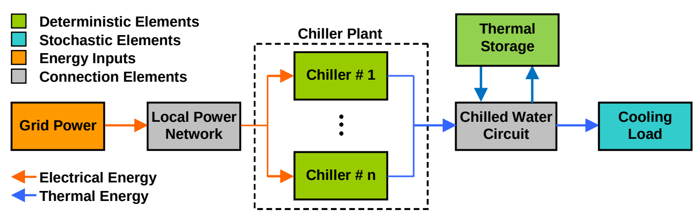


Fig. 1. Configuration of the building cooling system with thermal storage.

The considered building cooling system has no local generation units and fully depends on the main distribution grid for the electric energy supply. The energy management problem consists in the minimization of the electric energy costs while guaranteeing at the same time an adequate comfort level in the zone. This is achieved by operating the chiller plant at optimal efficiency, suitably dispatching the individual chillers, and exploiting the thermal storage unit to put cooling energy aside for later usage. The presence of the storage element releases the chiller plant from strict load following, thus allowing it to operate at efficient regimes and in time slots where the electrical energy prices are lower. The resulting cooling power request mismatches are then compensated for by the storage unit. Further flexibility is added to the control problem by allowing small and time-limited modulations of the zone temperature set-point. This results in a temporary decrease of the cooling power request, at an affordable cost in terms of reduction of the comfort level.

The envisaged energy management problem can be formalized as a constrained stochastic optimal control problem for a Stochastic Hybrid System (SHS). In analogy with [2], it is also convenient to hierarchically decouple the problem into two separate optimization tasks, one related to the chiller plant operation and the other concerning the energy management of the storage. The former amounts to a static nonlinear optimization problem, aiming at optimally distributing the given power request among the various chillers of the plant. Then, a Dynamic Programming (DP) stochastic optimization problem is formulated to optimally distribute the cooling power request to the chiller plant and to the thermal storage unit. The

*This work is partly supported by the European Commission under the UnCoVerCPS project, grant number 643921. The work was carried out while M. Strelec was with Honeywell Prague Laboratory, Czech Republic.

[1]R. Vignali, F. Borghesan, L. Piroddi, and M. Prandini are with the Dipartimento di Elettronica, Informazione e Bioingegneria, Politecnico di Milano, Italy ({riccardomaria.vignali, luigi.piroddi, maria.prandini}@polimi.it, francesco.borghesan@mail.polimi.it)

[2]M. Strelec is with New Technologies for the Information Society - European Centre of Excellence, Faculty of Applied Sciences, University of West Bohemia, Pilsen, Czech Republic (strelec@ntis.zcu.cz)

possibility of modulating the cooling power request by acting on the temperature set-point is also exploited in the latter optimization problem.

An approximate solution to the *stochastic* DP problem is here pursued, which is based on the abstraction of the underlying SHS to a controlled Markov Chain (MC) with costs associated to transitions computed through appropriately defined simulations of the original hybrid system. The idea of adopting a finite approximate abstraction of the system to address the DP solution is inspired by the hierarchical approach in [3]. A key difference with that work is the use of SHSs, for which only few results are available regarding the design of approximate abstractions with provable approximation guarantees [4], [5], [6], [7], [8].

It is worth mentioning that similar energy management problems have been addressed in the literature mainly using Model Predictive Control (MPC) techniques, [9], [10], or focusing on a one-day horizon planning and solving the corresponding finite-horizon optimization problem, [11], [12]. Deterministic approaches using MPC and scheduling techniques have been explored, e.g., in [13], [14], [15], [16], [17], [18], [19]. also in a distributed set-up, [20], [21]. Stochastic approaches based on stochastic MPC techniques resting on sampling of possible scenarios are adopted in, e.g., [22], [23], [12]. The approach pursued herein is based instead on a DP formulation. This allows to compute the control policy off-line and to account for nonlinear stochastic dynamics comprising also discrete variables. The availability of a pre-computed control policy greatly simplifies the on-line implementation of the control strategy. In addition, a side result of the policy computation is the expected value of the achievable performance, which provides a convenient way to quantify it in advance. The achieved results are indeed significant in general, irrespectively of the considered application framework. Various problems in control –as well as safety analysis and verification– can be formally stated as stochastic DP problems, [24], [25]. DP offers directly a feedback solution, without requiring the on-line re-computation of the control input to counteract uncertainty as is the case with MPC, where simplified linear models are typically introduced to enable fast computations. Still, DP equations are rarely solvable exactly when continuous state systems are involved and Approximate DP (ADP) solutions are needed, [26]. ADP methods have been extensively investigated in the literature, and here we are able to find an efficient solution by exploiting a finite abstraction of the system and the parallelizable structure of the problem.

This work is the final result of a long-term research project, of which the conference papers [2], [27], and [28] represent various development stages. Each of them deals with one specific aspect, e.g., optimal energy management of a building with two chiller units, presence of stochastic inputs and multiple chillers to orchestrate, and availability of a thermal storage for operating the chillers at high efficiency by shifting the load in time. The present paper extends in a non trivial way the work in these papers by investigating a comprehensive setting that includes all aspects together. This implies a non-straightforward elaboration of the main methodology first introduced in [2], which sets the control problem formulation and its decomposition, but is restricted to a deterministic setting where disturbances assume their nominal profiles and to a cooling system without storage, which limits the DP challenge to setting a scalar input. A stochastic framework is considered in [27] but still in the simple configuration without thermal storage.
The contribution that is closest to this paper is [28], where the thermal storage is present. The introduction of the storage unit has a relevant impact on the control problem formulation, adding flexibility but making the DP formulation more complex. Further state and input variables are introduced, which makes the control policy definition and the DP equations solution more challenging. With respect to the preliminary work [28], a neater and more detailed formal setting is provided here, theoretical results are not only sketched but formally derived, including all mathematical derivations. Furthermore, the chiller optimization problem is generalized to the case of more than 2 chillers, conceiving an iterative procedure that optimizes a single parameter per iteration and ends in a number of steps equal to the number of chillers minus one. Finally, the policy calculation is performed efficiently using a parallel implementation of the ADP solution on a Graphics Processor Unit (GPU). This is indeed a less eye-catching aspect of the paper, but nonetheless decisive. Indeed, the proposed methodology, while computationally intensive, lends itself to this kind of heavy parallelization, which overall makes the presented approach feasible.

An extensive simulation study has been carried out for this work, using this efficient version of the code that exploits the parallelizable structure of the method. A Monte Carlo analysis of the performance is included, also comparing the presented method with a smart heuristic.

A simple –yet meaningful– model setting is employed in this work, considering a simplified thermal model of the zone, without modeling the energy accumulation properties of the walls. Indeed, the main interest here is on how the control system can respond to an aggregate load request. Adding the wall dynamics would only complicate the technical derivation, without affecting the main control design methodology. In some recent work [11], following [29], [30], we introduced a detailed building model with multiple layers walls subject to radiation, convection, and conduction heat transfer, and show how the building can be exploited as a passive storage. The resulting model is however high dimensional, with state variables that are hardly measurable, and classical model reduction techniques are applied to make it easier to handle and to integrate with further micro-grid components for energy management purposes. In turn, low level controllers are not explicitly modeled in [11] so as to obtain a linear-in-the-control-variables (though high dimensional) model. Based on this linear model, a compositional modeling framework oriented to the energy management of a district network is presented in [31], where multiple buildings are considered that share resources so as to minimize operation and maintenance costs. The direct compensation of disturbances according to a randomized strategy is studied in [12], still based on the model in [11].

The rest of the paper is structured as follows. A detailed description of the building cooling system under consideration is provided in Section II, together with a model of the stochastic disturbances. Section III formulates the constrained stochastic optimization problem, briefly recalling the results in [2] on its decomposition into chiller plant optimization and modulation of the cooling power request to the chiller and of the zone temperature set-point. Section IV addresses the chiller plant optimization problem, whereas Section V deals with the DP approach to the zone temperature set-point and chiller cooling power request modulation problems, as well as the ADP solution based on the Markov chain abstraction. Section VI discusses implementation aspects of the ADP solution and, in particular, its parallel GPU implementation. Section VII presents the results obtained in a numerical instance of the building cooling system case study, and includes a comparative statistical analysis of performance with respect to a smart heuristic. Finally, in Section VIII we draw some conclusions and briefly discuss possible extensions of this work.

## II. System description

We shall next describe the components of the considered system, which is schematically represented in Fig. 1.

### A. Plant model

*1) Grid and Local Power Network:* The system of Fig. 1 does not include any electric generator unit, neither renewable nor traditional, and we assume that the main grid, by way of the Local Power Network (LPN), provides to the chillers the exact amount of electric power required to satisfy the cooling load demand, *i.e.*:

$$P_g = \sum_{i=1}^{n} P_{e,i}, \tag{1}$$

where $P_g$ is the grid power, and $P_{e,i}$ is the electric power requested by the $i$th chiller, $i = 1, \ldots, n$.

*2) The chilled water circuit:* The chilled water circuit (CHWC) is composed of three sections, associated to the cooling load, the chiller plant and the thermal storage, respectively, and characterized by the mass flows $w_{pipe}$, $w_{ch}$, and $w_{st}$ (see Fig. 2). An identical mass flow variable $w_{st}$ is assumed to characterize both the inlet and the outlet of the thermal storage, which is operated at constant volume. By construction,

$$w_{pipe} = w_{ch} + w_{st}.$$

Both the chiller plant and the thermal storage unit can provide cooling energy to the load (when $w_{st} > 0$). On the other hand, if $w_{st} < 0$ the thermal storage is absorbing part or all the cooling power produced by the chillers. The other mass flow variables are assumed non-negative.

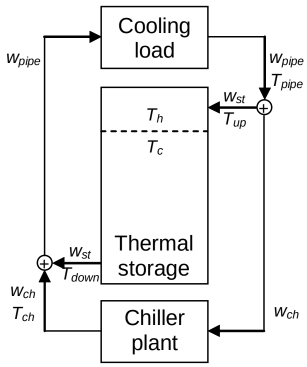


Fig. 2. Scheme of the CHWC.

The temperature at the outlet of the chiller plant is denoted $T_{ch}$, while $T_{pipe}$ is the temperature at the outlet of the cooling load.

*3) The cooling load:* The cooling load associated with the thermal control of the zone is described through the evolution of its temperature $T_z$:

$$C_z \frac{dT_z}{dt} = -Q_z + Q_i + k_{out}(T_a - T_z), \tag{2}$$

where $T_a$ (outside ambient temperature) and $Q_i$ (internal heat gain) are disturbances affecting the system, while

$$Q_z = X_z k_{cw}(T_z - T_{pipe})$$

is the heat power released to the CHWC, $X_z \in [0,1]$ being the fraction of available cooling power that is actually provided to the zone, as determined by the thermostat controller (see Section II-B). In the previous expressions $k_{out}$ and $k_{cw}$ are heat transfer coefficients, and $C_z$ is the thermal capacity of the zone.

**Remark 1** *Note that we consider a simplified thermal model of the zone, that does not account for the energy accumulation properties of the walls. Adding the wall dynamics would further complicate the model, highly increasing its dimensionality by introducing not directly measurable state variables associated with the temperature of the wall layers, [11], [30], [29]. Some observer should then be put in place to obtain an estimate of the state for implementing the policy. Given that this would make the argumentation more involved without adding interesting aspects to the problem, we adopt the simpler model (2).*

*4) The chiller plant:* The cooling power $Q_c$ requested to the chiller plant is split between the $n$ chillers according to

$$Q_{c,i} = \alpha_i^\circ Q_c, \tag{3}$$

where $\alpha_i^\circ$, $i = 1,\ldots,n$, are parameters defining the individual chiller commitment, that take values in $[0,1]$ and add up to 1, *i.e.* $\sum_{i=1}^n \alpha_i^\circ = 1$. Notice that the individual chillers have specific bounds on the maximum suppliable cooling power, so that the cooling power $Q_{c,i}$ requested to the $i$th chiller must satisfy $0 \le Q_{c,i} \le Q_{c,i}^{\max}$.

In terms of electric power consumption, one must also consider the activation status of the chillers. More precisely, if chiller $i$ is off, then $P_{e,i} = 0$. On the contrary, if the $i$th chiller is activated, then the electric power $P_{e,i}$ required to produce $Q_{c,i}$ can be computed according to the nonlinear static Gordon-Ng model, [1], [32]:

$$P_{e,i} = \frac{a_{i,1}T_aT_{pipe} + a_{i,2}(T_a - T_{pipe}) + a_{i,4}T_aQ_{c,i}}{T_{pipe} - a_{i,3}Q_{c,i}} - Q_{c,i}, \tag{4}$$

$a_{i,k}$, $k = 1,\ldots,4$, being suitable (empirically determined) coefficients. Notice that $P_{e,i}$ is not exactly 0 if $Q_{c,i} = 0$, since a small amount of power is still necessary to keep the chiller on. Here, the on/off status of the chillers is modeled implicitly through the commitment variables $\alpha_i^\circ$ (when $\alpha_i^\circ = 0$, then, chiller $i$ is off), *i.e.*

$$P_{e,i} = \begin{cases} \frac{a_{i,1}T_aT_{pipe} + a_{i,2}(T_a - T_{pipe}) + a_{i,4}T_a\alpha_i^\circ Q_c}{T_{pipe} - a_{i,3}\alpha_i^\circ Q_c} - \alpha_i^\circ Q_c, & \alpha_i^\circ \neq 0 \\ 0, & \alpha_i^\circ = 0, \end{cases} \tag{5}$$

which is derived by combining (3) and (4).

The efficiency of the chiller plant can be characterized through the Coefficient Of Performance

$$COP = \frac{Q_c}{\sum_{i=1}^n P_{e,i}}, \tag{6}$$

and the parameter vector $\alpha^\circ = (\alpha_1^\circ, \alpha_2^\circ, \ldots, \alpha_n^\circ) \in [0,1]^n$ defining the individual chiller commitment via (3) must be properly designed to ensure an optimal operation of the chiller plant for any given power request $Q_c$.

*5) The thermal storage:* A two-level stratified model is adopted for the thermal storage [33], where the (cold) lower block is at temperature $T_c$ and the upper (warm) one at temperature $T_h$. The cooling energy accumulated in the storage depends on the height $h_c$ of the cold block, since it is given by $\rho A_{st} h_c c_p (T_h - T_c)$, where $\rho$ and $c_p$ are the water specific density and heat capacity, and $A_{st}$ is the cross-section area of the storage. Assuming that the total volume of water in the storage is constant, $h_c$ satisfies $\dot{h}_c = -w_{st}/(\rho A_{st})$, where $w_{st}$ denotes the flow through the storage.

In the charging phase ($w_{st} < 0$), the lower block at temperature $T_c$ is fed by a flow at temperature $T_{down} = T_{ch}$, and the outflow from the upper block is at temperature $T_{up} = T_h$. In the discharging phase ($w_{st} > 0$), the upper block at temperature $T_h$ is fed by a flow at temperature $T_{up} = T_{pipe}$, and the outflow from the lower block is at temperature $T_{down} = T_c$.

Assuming that $T_{ch}$ is controlled to a constant set-point, and that the heat exchange between the two blocks can be neglected, the lower block stores and releases cold water at $T_c = T_{ch}$, so that the left-hand-side of the CHWC can be assumed to be at temperature $T_{ch}$. Similarly, provided that $T_{pipe}$ is controlled to some constant set-point, the right-hand-side of the CHWC can be assumed to be at temperature $T_{pipe}$. This assumption, together with the condition $w_{pipe} = w_{ch} + w_{st}$ on the flows in the CHWC, leads to:

$$C_{pipe}\frac{dT_{pipe}}{dt} = c_p w_{pipe}(T_{ch} - T_{pipe}) + Q_z,$$
$$C_{ch}\frac{dT_{ch}}{dt} = c_p w_{ch}(T_{pipe} - T_{ch}) - Q_c,$$

where $C_{pipe}$ and $C_{ch}$ are thermal capacities, $Q_z$ is the heat power absorbed from the zone, and $Q_c$ the cooling power provided by the chiller plant.

## B. Low-level control scheme

The control system is structured in a hierarchical two-level scheme, where the lower level is in charge of various temperature control tasks (concerning $T_{ch}$, $T_{pipe}$, and $T_z$), while the higher level (*supervisor*) addresses the optimal energy management problem. Fig. 3 represents the low-level portion of the control scheme of the system under consideration:

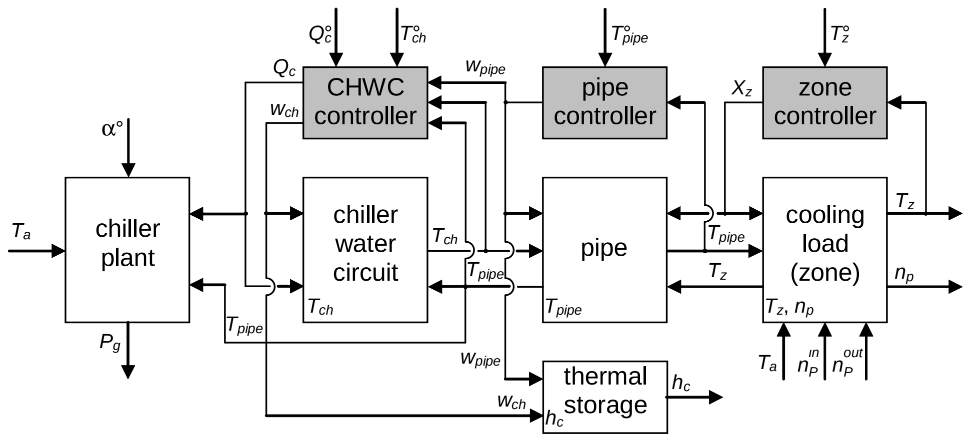


Fig. 3. Detailed low-level control scheme of the building cooling system.

*1) Water circuit temperature controller:* Temperature $T_{pipe}$ is kept at the set-point $T^\circ_{pipe}$ by means of a PI controller acting on $w_{pipe}$[1]:

$$w_{pipe} = k_p^{pipe}(T_{pipe} - T^\circ_{pipe}) + k_i^{pipe}\int (T_{pipe} - T^\circ_{pipe})dt.$$

Keeping $T_{pipe}$ at some constant value $T^\circ_{pipe}$ facilitates the stratification in two blocks of the thermal storage and the efficient operation of the chiller plant at some constant regime.

*2) Zone temperature controller:* Similarly, another PI controller keeps temperature $T_z$ at the set-point $T^\circ_z$ acting on $X_z$. More specifically, variable $X_z$ is set to 0 when zone cooling is de-activated. Otherwise, it is determined by the following equation:

$$X_z = k_p^z(T_z - T^\circ_z) + k_i^z\int (T_z - T^\circ_z)dt,$$

To properly account for the saturation of variable $X_z$ an anti-windup implementation of the PI controller is actually adopted.

*3) Chilled water temperature controller:* Temperature $T_{ch}$ is maintained at some constant set-point $T^\circ_{ch}$ through the following switching control scheme. If the storage is not available, then $w_{st} = 0$ (and, hence, $w_{ch} = w_{pipe}$) and $T_{ch}$ is kept at $T^\circ_{ch}$ by a PI controller with disturbance compensation acting on $Q_c$:

$$Q_c = k_p^{ch}(T_{ch} - T^\circ_{ch}) + k_i^{ch}\int (T_{ch} - T^\circ_{ch})dt + w_{ch}c_p(T_{pipe} - T^\circ_{ch}).$$

Otherwise, the chiller plant is assigned some (constant) cooling power request $Q^\circ_c \in [0, Q_c^{\max}]$, where $Q_c^{\max} = \sum_{i=1}^n Q_{c,i}^{\max}$ is the maximum cooling power that the chiller plant can supply, and the storage eventually compensates for the residual cooling power needed to keep $T_{ch}$ equal to $T^\circ_{ch}$. In the latter case, the flow through the chiller plant would be given by

$$w_{ch} = w^\circ_{ch} = k_p^{w_{ch}}(T^\circ_{ch} - T_{ch}) + \frac{Q^\circ_c}{c_p\left(T_{pipe} - T^\circ_{ch}\right)},$$

thus requiring a flow $w_{st} = w^\circ_{st} = w_{pipe} - w^\circ_{ch}$ through the storage. If we denote by $h_{st}$ the height of the storage, then its availability can be expressed by the binary variable $a_{st} = (0 < h_c < h_{st}) \vee (h_c = h_{st} \wedge w^\circ_{st} \geq 0) \vee (h_c = 0 \wedge w^\circ_{st} \leq 0)$, which is true if one of these conditions is satisfied:

a) the storage is neither completely full nor completely empty,
b) it is full and a release of cold flow is requested,
c) it is empty and acceptance of cold inflow is requested.

Note that the adopted switching logic encompasses the constraint $0 \leq h_c \leq h_{st}$, which can be therefore omitted in the optimal energy management problem formulation.

[1]The error sign is defined so as to obtain positive controller gains.

## *C. Model of the disturbances*

The building cooling system is subject to two disturbances, *i.e.*, the internal heat gain and the outside ambient temperature. In this work, the internal heat gain $Q_i$ is modeled as suggested in [11], that is:

$$Q_i = \left[a_1 T_z^2 + a_2 T_z + a_3\right] n_P + Q_i^+. \tag{7}$$

The first term represents the contribution of the zone occupants to the heat production and is given by the product of the heat generated by a single person with the number $n_P$ of occupants of the zone according to an empirical model documented in [34]. The second term accounts for other types of heat sources that may affect the internal energy of a building, e.g., lighting, electrical equipment, daylight radiation through windows and can be modeled as

$$Q_i^+ = \kappa n_P + \chi + \eta Q^S.$$

The thermal energy contribution due to internal lightening and electrical equipment is composed of two terms: a constant term $\chi$, and an additional term $\kappa n_P$ that represents the change in internal lightening and electrical equipment when people are present and is proportional to occupancy. The contribution of daylight radiation through windows is proportional to the solar radiation $Q^S$ through some coefficient $\eta$ that takes into account the mean absorbance coefficient of the zone, the transmittance coefficients of the windows and their areas, sun view and shading factors, and radiation incidence angle. Accurate forecasts can be obtained for the solar radiation and sensor measurements might be available for directly compensating it, [12]. We here consider the solar radiation as a deterministic signal.

We instead model the occupancy as a stochastic variable. Occupants constitute a significant source of heating in densely occupied buildings, such as offices and shops, and, due to the improved building thermal insulation, they are becoming an even more important factor. Parameter $n_P$ is modeled through a birth-death process with time varying birth (arrivals) and death (departure) rates, $\lambda_{in}(t)$ and $\lambda_{out}(t)$, respectively. Such rates are designed so that the resulting average occupancy matches some reference profile.

This can be viewed as a generalization of the model in [35], where a *Markov chain* is employed to model a single occupant.
It is assumed that the building is inhabited only during the day and people start entering the building at a specified time $t_{in}$. Accordingly, we define $n_P$ as follows:

$$n_P(t) = \max\left(n_P^{in}[t_{in}, t] - n_P^{out}[t_{in}, t], 0\right),$$

where $n_P^{in}[t_{in}, t]$ and $n_P^{out}[t_{in}, t]$ are independent Poisson processes representing respectively the number of arrivals and departures within $[t_{in}, t]$. The time-varying rates $\lambda_{in}(\cdot)$ and $\lambda_{out}(\cdot)$ of $n_P^{in}[t_{in}, t]$ and

$n_P^{out}[t_{in},t]$ are defined based on a nominal occupancy profile $\bar{n}_P$ which is nonzero in a given time interval $[t_{in},t_{out}]$. Specifically, observing that

$$E\left[n_P^{in}[t_{in},t]-n_P^{out}[t_{in},t]\right]=\int_{t_{in}}^{t}\lambda_{in}(\eta)d\eta-\int_{t_{in}}^{t}\lambda_{out}(\eta)d\eta,$$

we define the rates within $[t_{in},t_{out}]$ based on the time derivative $\dot{\bar{n}}_P$ of the nominal occupancy profile as follows:

$$\lambda_{in}=\begin{cases}\dot{\bar{n}}_P, & \dot{\bar{n}}_P>0\\ 0, & \dot{\bar{n}}_P\leq 0\end{cases}\qquad \lambda_{out}=\begin{cases}-\dot{\bar{n}}_P, & \dot{\bar{n}}_P<0\\ 0, & \dot{\bar{n}}_P\geq 0.\end{cases}$$

Further, after $t_{out}$, the $\lambda_{out}$ rate is set to a sufficiently high value so as to guarantee with probability 0.99 that the building is empty within one hour. Fig. 4 plots some realizations of $n_P$ given some nominal profile $\bar{n}_P$.

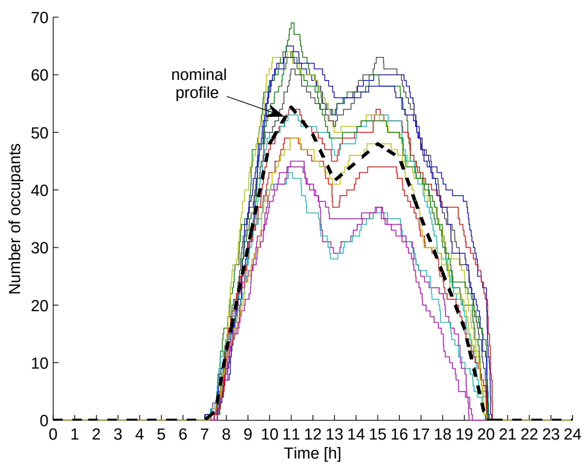


Fig. 4. Some realizations of the occupancy profiles. The nominal profile with $[t_{in},t_{out}]=[7,20]$ is represented as a dashed line. Different colors are used to distinguish different realizations.

The outside temperature $T_a$ is assumed to be given by some accurate forecast and treated as a deterministic signal. Indeed if the insulation level of the building is high, fluctuations around the forecast value have a limited impact and the effect of the internal heat gain is dominant.

### D. Interpretation as a stochastic hybrid system

The described system is stochastic since it is affected by stochastic disturbances ($n_P^{in}$, $n_P^{out}$), and hybrid since it comprises both continuous state variables and discrete state variables. More precisely, the continuous and discrete state components are given by $x=[T_z\ T_{ch}\ T_{pipe}\ w_{pipe}\ X_z\ Q_c\ h_c]^T$ and $q=n_P$ and take values in $\mathscr{X}=\mathbb{R}^4\times[0,1]\times[0,Q_c^{\max}]\times[0,h_{st}]$ and $\mathscr{Q}=\mathbb{Z}_{\geq 0}$, respectively. The evolution in time of the hybrid state $(x,q)$ is governed by the equations described in the previous subsections, and is affected by the disturbances $n_P^{in}$, $n_P^{out}$ and $T_a$, and by the control inputs $Q_c^\circ$, $T_{ch}^\circ$, $T_{pipe}^\circ$, $T_z^\circ$, and $\alpha^\circ$. Of the latter, the set-points $T_{ch}^\circ$ and $T_{pipe}^\circ$ are pre-assigned and are not object of the subsequent control design for optimal energy management. As for the zone temperature set-point $T_z^\circ$, it is given by $T_z^\circ=\bar{T}_z+\Delta_z^\circ$, where $\Delta_z^\circ\in[0,\Delta_{\max}]$ represents the allowed variation with respect to some reference set-point value $\bar{T}_z$ and is used to save energy. Energy saving comes at the price of causing some discomfort. Given the control horizon $[t_0,t_f]$, we then introduce the state variable

$$d(t)=\int_{t_0}^{t}\Delta_z^\circ(t)dt,\ t\geq t_0,$$

to quantify the discomfort within $[t_0,t]$, and avoid that it exceeds some maximum admissible value $d_{\max}$

$$d(t)\leq d_{\max},\ t\in[t_0,t_f].$$

**Remark 2** *The underlying implicit assumption here is that $T_z^\circ$ is representative of the actual behavior of $T_z$ (*i.e.*, the lower-level controllers have been appropriately designed so as to guarantee a satisfactory tracking performance) while $\bar{T}_z$ is an ideal temperature as for the occupants comfort. In this way, if $d_{\max}=0$, then, no discomfort is introduced.* □

The hybrid state is hence enlarged so as to include the continuous variable $d$, *i.e.* $s=(d,x,q)$, and takes values in the hybrid state space $\mathscr{S}=[0,d_{\max}]\times\mathscr{X}\times\mathscr{Q}$. The control inputs for addressing the optimal energy management problem are $\alpha^\circ\in[0,1]^n$, $\Delta_z^\circ\in[0,\Delta_{\max}]$, and $Q_c^\circ\in[0,Q_c^{\max}]$.

## III. Optimal energy management

The energy management supervisor of the building cooling system with thermal storage should act on the control inputs $\alpha^\circ\in[0,1]^n$, $\Delta_z^\circ\in[0,\Delta_{\max}]$, and $Q_c^\circ\in[0,Q_c^{\max}]$ so as to minimize the average electric energy cost spent over a given time horizon $[t_0,t_f]$, while not exceeding the maximum discomfort level $d_{\max}$ caused by the zone temperature set-point modulation. This can be formulated as a finite-horizon stochastic optimal control problem, as explained hereafter.

Let

$$\pi:\mathscr{S}\times[t_0,t_f]\to[0,1]^n\times[0,\Delta_{\max}]\times[0,Q_c^{\max}]$$

be a state-feedback control policy that maps a state-time pair $(s,t)$ into some values for the commitment parameters $\alpha^\circ$, and the set-points $\Delta_z^\circ$ and $Q_c^\circ$ to be applied at time $t$ when the state value is equal to $s$. Then, the goal is to find a policy that is optimal by solving the following constrained stochastic optimization problem:

$$\min_{\pi} E_{s_0}^{\pi}\Big[\int_{t_0}^{t_f}c_g(t)P_g(t)dt\Big] \tag{8}$$
$$\text{subject to: } d(t)\leq d_{\max},\forall t\in[t_0,t_f],$$

where $P_g(t)=\sum_{i=1}^{n}P_{e,i}(t)$ denotes the power requested to the main distribution grid and $c_g(t)$ is the price per unitary power request, at time $t\in[t_0,t_f]$.

Here, $s_0$ is the state value at time $t_0$ and $E_{s_0}^{\pi}$ denotes the expected value when the initial state is $s_0$ and the control policy $\pi$ is applied. Indeed, different initial state values and/or control policies induce different probability distributions over the system trajectories and, as a consequence, over the realizations of the stochastic process $P_g(t)$. Notice that, if the energy price $c_g(t)$ is taken to be constant, one is actually minimizing the average electric energy consumption.

The problem of designing the control policy $\pi$ can be decomposed into two subsequent phases:

1) design $\pi_{\alpha^\circ}:\mathscr{S}\times[t_0,t_f]\to[0,1]^n$ for the chillers commitment, and
2) based on the outcome of phase 1, design $\pi_{\Delta_z^\circ Q_c^\circ}:\mathscr{S}\times[t_0,t_f]\to[0,\Delta_{\max}]\times[0,Q_c^{\max}]$ for the modulation of the zone temperature and chiller cooling power request set-points.

The policy $\pi$ is then obtained by combining these two maps, *i.e.* $\pi=(\pi_{\alpha^\circ},\pi_{\Delta_z^\circ Q_c^\circ})$, and is actually optimal if $\pi_{\alpha^\circ}$ is designed so as to minimize the electric power requested to provide a certain cooling energy, and, in turn, policy $\pi_{\Delta_z^\circ Q_c^\circ}$ is designed so as to minimize the average electric energy cost when the chillers commitment is determined by the policy $\pi_{\alpha^\circ}$ obtained in the first phase.

Indeed, the rationale behind the decomposition of the policy optimization is that, given a cooling power request $Q_c$ to the chiller plant, its dispatching among the individual chillers affects only the electric power demand $P_g=\sum_{i=1}^{n}P_{e,i}$, whereas it has no influence on the dynamics of the zone and chiller water circuit temperatures. Now, $P_g$ is a static function of $\alpha_i^\circ$, $i=1,\ldots,n$, $Q_c$, $T_{pipe}$, and $T_a$ (see (5)).

Therefore, since $Q_c$, $T_{pipe}$, and $T_a$ are independent of $\alpha_i^\circ$, one can design the optimal commitment strategy as follows:

$$\alpha_i^\star(Q_c,T_a,T_{pipe}) = \arg\min_{\alpha_i^\circ} P_g.$$

This amounts to solving a (nonlinear) static optimization problem (see Section IV). The resulting $\alpha_i^\star(Q_c,T_{pipe},T_a)$ implicitly defines the optimal map $\pi^\star_{\alpha^\circ}$. Indeed, $\alpha_i^\star(Q_c,T_{pipe},T_a)$ can be viewed as a time-varying function of the state $s \in \mathscr{S}$, observing that $T_{pipe}$ and $Q_c$ are state variables, the time variability being induced by $T_a$.

The map $\pi_{\Delta_z^\circ Q_c^\circ} : \mathscr{S} \times [t_0,t_f] \to [0,\Delta_{\max}] \times [0,Q_c^{\max}]$ for the modulation of the zone temperature and chiller cooling power request set-points can then be designed by solving the constrained optimization problem:

$$\begin{aligned} &\min_{\pi_{\Delta_z^\circ Q_c^\circ}} E_{s_0}^{\pi_{\Delta_z^\circ Q_c^\circ}} \Big[ \int_{t_0}^{t_f} c_g(t) P_g^\star(t) dt \Big] \qquad (9) \\ &\text{subject to: } d(t) \le d_{\max},\, t \in [t_0,t_f], \end{aligned}$$

where $P_g^\star(t)$ is the power demand when the optimal commitment policy $\pi^\star_{\alpha^\circ}$ obtained in phase 1 is used to define the individual chiller commitment coefficients $\alpha^\circ$. Problem (9) will be tackled via ADP in Section V.

As a result of the problem decomposition, the energy management system is composed of two blocks, *i.e.*, the *chiller plant optimizer*, which decides how the requested cooling power should be split among the chillers, and the *optimal set-point modulator*, which determines the actual cooling power requests to the chiller plant and storage by acting on the zone temperature and the chiller power set-points (see Fig. 5).

Note that the advantage of decomposing the problem into chiller plant optimization and optimal set-point modulation is twofold: 1) we obtain a computational procedure to find a solution to the overall energy management optimization problem (8); and 2) we have to solve two lower-dimensional optimization problems (one static and the other dynamic) in place of a large (dynamic) optimization problem.

A further practically relevant benefit of this decomposition is that we can also address the case when the strategy adopted for the chillers commitment is given, and only the set-point modulation is possible. We just need to solve problem (9) with the electric power consumption as determined by the assigned chillers commitment strategy.

## IV. Chiller Plant Optimizer

Our objective is to design the chiller plant optimizer that splits the cooling power request $Q_c$ between the $n$ chillers so as to optimize the overall performance of the chiller plant, measured in terms of the electric power consumption $P_g$ needed to satisfy a given cooling power request. Recall now that $P_g$ is given by equation (1), where $P_{e,i}$ is the energy power needed by the $i$th chiller to provide the cooling power $Q_{c,i} = \alpha_i^\circ Q_c$.

Since each $P_{e,i}$ is given by (5), then, the optimal commitment $\pi^\star_{\alpha^\circ} : \mathscr{S} \times [t_0,t_f] \to [0,1]^n$ can be obtained by solving for each triplet ($Q_c$, $T_a$, $T_{pipe}$) the following nonlinear static optimization problem with $n$ optimization variables:

$$\begin{aligned} &\min_{\alpha_i^\circ,\, i=1,\dots,n} \sum_{i=1}^n P_{e,i}[\alpha_i^\circ Q_c] \qquad (10) \\ &\text{subject to:} \\ &0 \le \alpha_i^\circ \le \frac{Q_{c,i}^{\max}}{Q_c},\; i=1,\dots,n \\ &\sum_{i=1}^n \alpha_i^\circ = 1 \end{aligned}$$

where the notation $P_{e,i}[\alpha_i^\circ Q_c]$ is adopted to point out the dependence of $P_{e,i}$ on $\alpha_i^\circ$ through $Q_{c,i} = \alpha_i^\circ Q_c$.

Note that the optimization problem (10) is difficult to solve when $n$ is large, since it is nonlinear and involves $n$ optimization variables. We next show how the solution to (10) can be found by solving $n-1$ nonlinear optimization problems involving a single optimization variable.

Let $n > 2$ and consider the following two optimization problems, both to be solved for each triplet ($Q_c$, $T_a$, $T_{pipe}$):

$$\begin{aligned} &\min_{\beta_i,\, i=1,\dots,n-1} \sum_{i=1}^{n-1} P_{e,i}[\beta_i Q_c] \qquad (11) \\ &\text{subject to:} \\ &0 \le \beta_i \le \frac{Q_{c,i}^{\max}}{Q_c},\; i=1,\dots,n-1 \\ &\sum_{i=1}^{n-1} \beta_i = 1, \end{aligned}$$

where $0 \le Q_c \le \sum_{i=1}^{n-1} Q_{c,i}^{\max}$, and

$$\begin{aligned} &\min_{\gamma_1} \left\{ P^\star_{e,[1,n-1]}[\gamma_1 Q_c] + P_{e,n}[\gamma_2 Q_c] \right\} \qquad (12) \\ &\text{subject to:} \\ &0 \le \gamma_1 \le \sum_{i=1}^{n-1} \frac{Q_{c,i}^{\max}}{Q_c} \\ &0 \le \gamma_2 \le \frac{Q_{c,n}^{\max}}{Q_c} \\ &\gamma_1 + \gamma_2 = 1 \end{aligned}$$

where $0 \le Q_c \le Q_c^{\max}$ and $P^\star_{e,[1,n-1]}[Q_c]$ represents the optimal value of the cost function in problem (11) involving chillers $1,\dots,n-1$, which are treated as if they were a single chiller plant in (12).

Now, denote by $\beta_i^\star[Q_c]$, $i=1,\dots,n-1$, and $\gamma_i^\star[Q_c]$, $i=1,2$, the solutions to (11) and (12), respectively. Let also $\alpha_i^\star[Q_c]$ be the optimal value of $\alpha_i^\circ$ obtained by solving (10). Then, the following proposition holds.

**Proposition 1**

$$\alpha_n^\star[Q_c] = \gamma_2^\star[Q_c] \qquad (13)$$

$$\alpha_i^\star[Q_c] = \gamma_1^\star[Q_c]\beta_i^\star\left[\gamma_1^\star[Q_c]Q_c\right],\; i=1,\dots,n-1. \qquad (14)$$

**Proof 1** *See the appendix.*

Observe now that the decomposition of problem (10) into the two optimization problems (11) and (12) corresponds to considering 2 chillers (chiller $n$ and an equivalent chiller obtained by grouping together the remaining $n-1$ chillers) and optimally dividing the load between them: fraction $\alpha_n^\star[Q_c])Q_c$ is assigned to chiller $n$ and $(1-\alpha_n^\star[Q_c])Q_c$ to the equivalent chiller. This same reasoning can be applied to the purpose of optimally dividing the fraction of load $(1-\alpha_n^\star[Q_c])Q_c$ assigned to the group of $n-1$ chillers, i.e., the $n-1$ chillers can be viewed as two chillers: chiller $n-1$ and an equivalent chiller obtained by grouping together the remaining $n-2$ chillers. By applying iteratively this reasoning, the optimal commitment parameters $\alpha_i^\star$, $i=1,\dots,n$, are finally effectively computed by solving $n-1$ optimization problems of the form (12), which can be done efficiently through gridding since each one of them involves a single optimization variable. Obviously, gridding introduces some approximation error, which makes the solution to the overall energy management problem sub-optimal. As the gridding gets finer and finer, however, the approximation error decreases and the optimal solution is recovered.

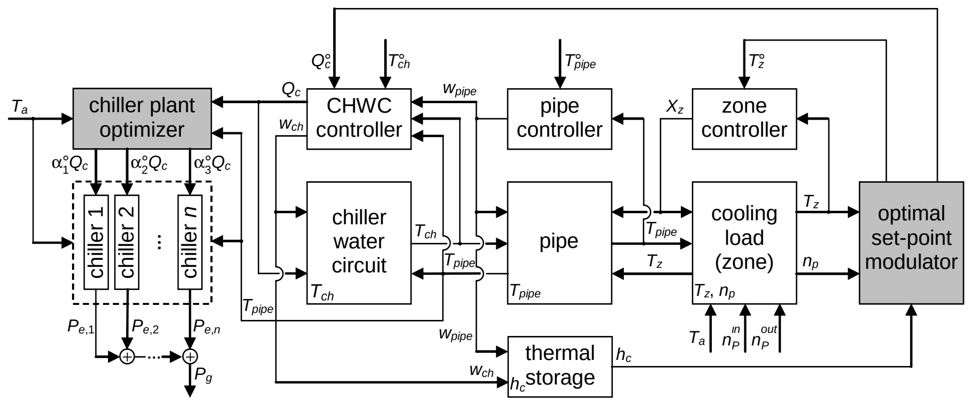


Fig. 5. Structure of the energy management supervisor.

## V. Optimal set-point modulator

Given the optimal chiller commitment policy designed in the previous section, our goal is to determine an optimal policy

$$\pi_{\Delta_z^\circ Q_c^\circ} : \mathscr{S} \times [t_0, t_f] \to [0, \Delta_{\max}] \times [0, Q_c^{\max}] \tag{15}$$

for the modulation of the set-points of the zone temperature and of the chiller cooling power request, which entails solving the constrained optimization problem (9). This is is a non-trivial task given the stochastic and hybrid nature of the system described in Section II, and is addressed here under the following assumption:

**Assumption 1** *The set-point signals $\Delta_z^\circ$ and $Q_c^\circ$ take values in finite sets, namely $\mathscr{U}_z$ and $\mathscr{U}_c$, and are updated every $\tau$ time instants.*

Assumption 1 is indeed a sensible one when aiming at a practical implementation of the optimal modulation policy. It also allows to rephrase the original problem as an analogous finite-horizon control problem for a discrete time SHS (dtSHS) with a control input $u = (u_z, u_c) = (\Delta_z^\circ, Q_c^\circ)$ taking values in the discrete control input set $\mathscr{U} = \mathscr{U}_z \times \mathscr{U}_c$. The executions of the dtSHS are obtained by sampling the executions of the original continuous time SHS with the control input $\Delta_z^\circ$ and $Q_c^\circ$ held constant over each time frame $[\tau_k, \tau_{k+1})$, $k = 0, \dots, N-1$, where $\tau_k = t_0 + k\tau$ and $N = \left\lceil \frac{t_f - t_0}{\tau} \right\rceil$. The values for $\Delta_z^\circ$ and $Q_c^\circ$ are determined by the discrete time policy $\nu = (\nu_0, \dots, \nu_{N-1})$ with

$$\nu_k : \mathscr{S} \to \mathscr{U}, \; k \in \{0, \dots, N-1\}, \tag{16}$$

which is optimized by solving the following constrained optimization problem:

$$\min_{\nu} E_{s_0}^{\nu} \Big[ \sum_{k=0}^{N-1} C_k(\bar{s}_k, \nu_k(\bar{s}_k), \bar{s}_{k+1}) \Big] \tag{17}$$
$$\text{subject to: } \bar{d}_k \le d_{\max}, k \in \{0, \dots, N\},$$

where we set

$$\bar{s}_k = s(\tau_k) \text{ and } \bar{d}_k = d(\tau_k)$$

as the sampled versions of the hybrid state and the discomfort variable, and

$$C_k(s, u, s') = \int_{\tau_k}^{\tau_{k+1}} c_g(t) P_g^\star(t) dt$$

is the energy cost associated to the continuous time SHS evolution in the time frame $[\tau_k, \tau_{k+1})$ from state $s(\tau_k) = s$ to state $s(\tau_{k+1}) = s'$ when the inputs $\Delta_z^\circ$ and $Q_c^\circ$ are held constant over $[\tau_k, \tau_{k+1})$ and set equal to $(\Delta_z^\circ(t), Q_c^\circ(t)) = u$, $t \in [\tau_k, \tau_{k+1})$.

Note that the evolution of the discomfort variable is given by

$$\bar{d}_{k+1} = \bar{d}_k + \Delta_z^\circ(\tau_k)\tau, \; \bar{d}_0 = 0, \tag{18}$$

where $\Delta_z^\circ(\tau_k)$ is the value of the component $u_z$ of the discrete input $u$ at time $k$. The state constraint in (17) can then be translated into a constraint on the admissible input values of the form

$$\nu_k(\bar{s}_k) \in U(\bar{s}_k), \; k \in \{0, \dots, N-1\},$$

where

$$U(s) = U(d, x, q) = \{u = (u_z, u_c) \in \mathscr{U} : d + u_z \tau \le d_{\max}\}. \tag{19}$$

The fact that the state constraint can be reformulated as a constraint on the admissible values for the control input $\Delta_z^\circ$ (based on the residual discomfort), allows to tackle the problem of determining the optimal policy $\nu^\star$ through DP techniques. In particular, $\nu^\star$ can be computed from the so-called $Q$-functions $Q_k : \mathscr{S} \times \mathscr{U} \to \Re_+$, $k = 0, \dots, N$, according to

$$\nu_k^\star(s) \in \arg\min_{u \in U(s)} Q_k(s, u), \; k = 0, \dots, N-1.$$

The Q-functions are computed via the following backward iterative procedure

$$Q_k(s,u) = E\left[ C_k(\bar{s}_k, u, \bar{s}_{k+1}) + \min_{u' \in U(\bar{s}_{k+1})} Q_{k+1}(\bar{s}_{k+1}, u') \Big| \bar{s}_k = s \right],$$
$$(s,u) \in \mathscr{S} \times \mathscr{U}, \; k = 0, \dots, N-1, \tag{20}$$

initialized at $k = N$ with $Q_N(s,u) = 0$, $(s,u) \in \mathscr{S} \times \mathscr{U}$.

The numerical solution to the DP equations (20) is hampered by the presence of continuous state components and of the expectation operator. The idea developed next is to find an Approximate DP (ADP) solution by abstracting the underlying SHS to a (finite state) controlled MC, whose transition costs are computed through appropriately defined simulations of the original SHS.

### *A. ADP solution based on MC abstraction*

In this section, the dtSHS introduced above is abstracted to an inhomogeneous controlled MC, which is defined by a triple $\{\mathscr{X}, \mathscr{A}, p\}$ where $\mathscr{X}$ is the state set, $\mathscr{A}$ the control set, and $p : \mathscr{X} \times \mathscr{A} \times \mathscr{X} \times \{0, \dots, N-1\} \to [0,1]$ is the controlled transition probability function. Specifically, $p(\hat{s}, a, \hat{s}', k)$ is the probability that a transition to $\hat{s}' \in \mathscr{X}$ occurs at $k \in \{0, \dots, N-1\}$ when the control input $a \in \mathscr{A}$ is applied from $\hat{s} \in \mathscr{X}$.

*1) Definition of the state and control sets:* Given that the control input to the MC is the same as in the original hybrid model, we have that $\mathscr{A} = \mathscr{U}$. As for the state $\hat{s}$ of the MC, it accounts only for the state variables $T_z$, $d$, $h_c$, $n_P$ of the dtSHS. The (discrete) state space $\mathscr{X}$ of the Markov chain approximation is determined as follows. We assume that, at each sample time $\tau_k$, $k = 1, \dots, N$, the zone temperature $T_z$ reaches the set-point value $T_z^\circ$ chosen at the previous sample time, so that $T_z$ ranges in a finite set, which is the set of admissible values for $T_z^\circ$. The storage height $h_c$ is quantized in the range $[0, h_{st}]$ with a gridding parameter $\delta h_{st}$, whereas $d$ takes values in some finite set as determined by the evolution in (18) of its sampled version and by the upper bound $d_{\max}$. The sampled number of occupants $n_P(\tau_k)$ of the dtSHS can take in principle arbitrarily high values and is constrained in some range which is computed based on an $\varepsilon$-coverage tube containing all possible occupancy profiles along $[t_0, t_f]$ except for a set whose probability is smaller than a user-defined value $\varepsilon \in [0,1]$.

*Computation of the $\varepsilon$-coverage tube:* The problem of determining the values taken by the component of the MC state $\hat{s}$ corresponding to $n_P$ is reformulated in terms of the following chance-constrained problem:

$$\min_{h_{1,k}\geq 0,\, h_{2,k}\geq 0,\, k=1,\ldots,N} \sum_{k=1}^{N} (h_{1,k}+h_{2,k}) \text{ subject to:} \tag{21}$$
$$P\{-h_{1,k} \leq n_P(\tau_k) - E[n_P(\tau_k)] \leq h_{2,k}, \forall k\} \geq 1-\varepsilon,$$

which can be solved through the scenario approach, [36].

The scenario solution rests on the extraction of $M$ profiles $n_P^{(i)}(t)$, $t \in [t_0, t_f]$, $i = 1, 2\ldots, M$, and on the solution of the following convex optimization problem:

$$\min_{h_{1,k}\geq 0,\, h_{2,k}\geq 0,\, k=1,\ldots,N} \sum_{k=1}^{N} (h_{1,k}+h_{2,k}) \text{ subject to:} \tag{22}$$
$$-h_{1,k} \leq n_P^{(i)}(\tau_k) - E[n_P(\tau_k)] \leq h_{2,k}, \forall k, i = 1,\ldots,M,$$

where the constraint in probability is replaced by its sampled version. If $M$ satisfies

$$\sum_{i=0}^{r-1} \binom{N}{i} \varepsilon^i (1-\varepsilon)^{N-i} \leq \beta,$$

where $r$ is the number of optimization variables and $\beta \in (0,1)$, then, the solution to (22) is feasible for the chance-constrained problem (21) with confidence larger than $1-\beta$.

*2) Definition of the transition probability function:* The probability $p(\hat{s}, u, \hat{s}', k)$ that the MC evolves from $\hat{s} = (\hat{d}, \hat{T}_z, \hat{h}_c, \hat{n}_P)$ at time $k$ to $\hat{s}' = (\hat{d}', \hat{T}_z', \hat{h}_c', \hat{n}_P')$ at time $k+1$ clearly depends on the control action $u \in \mathscr{U}$ applied at time $k$, and is zero if $\hat{s}'$ is not admissible as next state.

In particular, $\hat{T}_z'$ must satisfy $\hat{T}_z' = \bar{T}_z + \Delta_z^\circ$ (since temperature $T_z$ is controlled to $T_z^\circ = \bar{T}_z + \Delta_z^\circ$) and $\hat{d}' = \hat{d} + \Delta_z^\circ \tau$ (based on (18)). As for the thermal storage height, $\hat{h}_c'$ must be the quantized value of $h_c(\tau_{k+1})$ obtained when the SHS evolves within $[\tau_k, \tau_{k+1}]$ from $T_z(\tau_k) = \hat{T}_z$, $d(\tau_k) = \hat{d}$, $h_c(\tau_k) = \hat{h}_c$, and $n_P(\tau_k) = \hat{n}_P$, with the other state variables set at consistent equilibrium values, subject to the constant control input $u_k = u$ and the disturbances, *i.e.* the outside ambient temperature $T_a$ forecast along $[\tau_k, \tau_{k+1}]$ and the occupancy profile obtained by linearly interpolating $n_P$ at $\tau_k$ with $n_P'$ at $\tau_{k+1}$ as suggested in [27].

If $\hat{s}'$ satisfies these conditions (*i.e.* it is admissible), then $p(\hat{s}, u, \hat{s}', k)$ equals the probability of having $n_P' - n_P$ arrivals/departures within $[\tau_k, \tau_{k+1}]$, otherwise it is set to zero. In order to have $p(\hat{s}, u, \hat{s}', k)$ well defined as a probability, *i.e.*, summing up to 1 when $\hat{n}_P'$ ranges within the $\varepsilon$-coverage tube, we assign to the extreme values for $\hat{n}_P'$ the probability associated to all arrivals/departures $\Delta_P$ within $[\tau_k, \tau_{k+1}]$ that will make $\hat{n}_P + \Delta_P$ either exceed $E[n_P(\tau_{k+1})] + h_{2,k+1}$ or go below $E[n_P(\tau_{k+1})] - h_{1,k+1}$.

Problem (17) then reduces to determining policy $\hat{\nu} = (\hat{\nu}_0, \ldots, \hat{\nu}_{N-1}) : \mathscr{X} \times [0, N-1] \to \mathscr{U}$ by solving

$$\min_{\hat{\nu}} E_{x_0}^{\hat{\nu}} \Big[ \sum_{k=0}^{N-1} \hat{c}_k(\hat{s}_k, \hat{\nu}_k(\hat{s}_k), \hat{s}_{k+1}) \Big] \tag{23}$$
$$\text{subject to: } \hat{d}_k \leq d_{\max},\; k \in \{0,\ldots,N\},$$

where $\hat{c}_k(\hat{s}, u, \hat{s}')$ is the cost associated to a transition from $\hat{s}$ to $\hat{s}'$ when the control input $u$ is applied at time $k$. This cost represents the electric energy cost for that transition and can be determined by simulating the original SHS within $[\tau_k, \tau_{k+1}]$ as described above when defining the admissible values for $\hat{h}_c'$.

Again, the constraint in (23) can be translated into a constraint on the admissible values for the control action

$$\hat{\nu}_k(\hat{s}_k) \in U(\hat{s}_k),\; k \in \{0,\ldots,N-1\},$$

where $U(s)$ is defined in (19).

The optimal policy for the MC can then be computed as follows

$$\hat{\nu}_k^\star(\hat{s}) \in \arg\min_{u \in U(\hat{s})} \hat{Q}_k(\hat{s}, u),$$

where $\hat{Q}_k : \mathscr{X} \times \mathscr{U} \to \Re_+$, $k = 0,\ldots,N$, are the Q-functions, which can be derived via the DP equations:

$$\hat{Q}_k(\hat{s}, u) = \sum_{\hat{s}' \in \mathscr{X}} p_k(\hat{s}, u, \hat{s}') [\hat{c}_k(\hat{s}, u, \hat{s}') + \min_{u' \in U(\hat{s}')} \hat{Q}_{k+1}(\hat{s}', u')],$$
$$(\hat{s}, u) \in \mathscr{X} \times \mathscr{U},\; k = 0,\ldots,N-1, \tag{24}$$

initialized at $k = N$ with $Q_N(\hat{s}, u) = 0$, $(\hat{s}, u) \in \mathscr{X} \times \mathscr{U}$.

Note that the $Q$-functions for the MC abstraction can be stored in a look-up table and their computation is easily performed based on the MC transition costs and probabilities.

Finally, the (sub)-optimal control policy for the dtSHS can be recovered as follows:

$$\nu_k(s) = \hat{\nu}_k^\star(\hat{s})$$

where $\hat{s} = (\hat{d}, \hat{T}_z, \hat{h}_c, \hat{n}_P) \in \mathscr{X}$ is obtained from $s = (d, x, q)$ with $x = [T_z\ T_{ch}\ T_{pipe}\ w_{pipe}\ X_z\ Q_c\ h_c]^T$ by extracting the components $(d, T_z, h_c, n_P)$ and approximating them with the closest value in $\mathscr{X}$.

## VI. Implementation of the ADP solution

The computation of the Q-function at each $k$-th iteration step can be summarized in the following three steps: a) computation of the cost $\hat{c}_k(\hat{s}, u, \hat{s}')$, b) computation of the expected value over the next states $x'$, and c) minimization with respect to the control action $u$. All these tasks involve repeating a basic calculation for all possible combinations of the arguments. For example, calculating the value of the cost $\hat{c}_k(\hat{s}, u, \hat{s}')$ requires simulating the original SHS over the $k$-th time interval $[\tau_k, \tau_{k+1}]$ starting from the initial condition $\hat{s}$, applying the control action $u$, and choosing $\hat{s}'$ as the final state value, and this task has to be repeated for all possible triplets $(\hat{s}, u, \hat{s}')$, typically resulting in a huge computational load.

Fortunately, the various repetitions of the basic calculation involved in the mentioned tasks are all independent of each other, which allows an efficient implementation with parallelized code. Actually, this turns out to be essential to deal effectively with medium/large scale problems as the one considered in this paper.

To exploit parallelization, we here employ GPU-accelerated computing, that is able to deal with multiple tasks simultaneously by exploiting the massively parallel architecture of a GPU. As a parallel computing platform, we choose the NVIDIA CUDA. A sketch of the CUDA architecture is given in Fig. 6: the atomic computation units (threads) are organized in batches (blocks) that are collected in a grid. The threads execute in parallel the same subroutine, called kernel. In the case of the cost computation, for example, we choose as a kernel the function that simulates the SHS and assign to each thread a different initial condition, so that multiple executions of the SHS are performed at the same time.

Overall, the solution of the DP equations is coded in a MATLAB script, containing a MEX interface that runs the CUDA code on an NVIDIA Tesla k20 GPU. To give an idea of the computational advantages that can be gained with this architecture, while a MATLAB script takes approximately 0.01 seconds to run one of the simulations required in the cost evaluation task, with reference to the numerical example described in Section VII, the CUDA procedure can run more than 80000 such simulations in half a second.

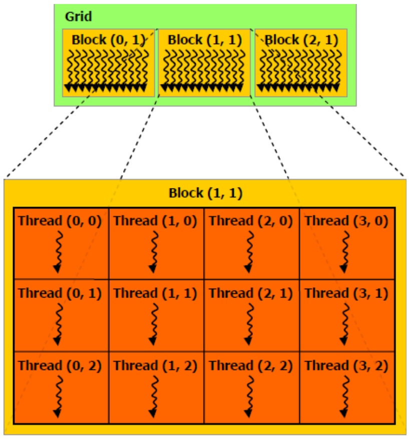


Fig. 6. Sketch of the CUDA architecture.

## VII. Numerical Example

The proposed ADP-based approach is applied to the energy management of a building cooling system along a one-day time horizon ($[t_0, t_f] = [0, 24]$ hours). The zone is occupied from 7:00 to 21:00, according to the stochastic occupancy profile described in Section II-C, and is cooled from 6:00 to 22:30 (the last control decision being taken at 22:00).

In the simulation study, we consider only the ambient temperature and occupancy as disturbance inputs, so as to ease the interpretation of the strategy implemented by the optimal policy. More specifically, in the internal heat gain (7) we consider only the contribution of the zone occupants to the heat production and neglect the additional $Q_{int}^{+}$ term that depends on the solar radiation.

The outside ambient temperature $T_a$ is given by the forecast in Fig. 7. Zone temperature set-point and cooling power request to the chiller plant can be changed every $\tau = 30$ minutes. We assume that $\Delta_z^\circ \in \mathcal{U}_z = \{0, \Delta_{\max}/2, \Delta_{\max}\}$, with $\Delta_{\max} = 1\,°C$ and $Q_c^\circ \in \mathcal{U}_c = \{k\,\delta Q_C : k = 0, \dots, 12\}$, where $\delta Q_c = 2$ kW. The maximum discomfort level is $d_{\max} = 6\,°C\,h$ corresponding to an increase of $1\,°C$ for 6 hours. The cost for the electrical energy is set to be constant and unitary ($c_g(t) = 1,\ t \in [0, 24]$), so that we are actually minimizing the energy consumption.

A list of the system parameter values is given in Table I.

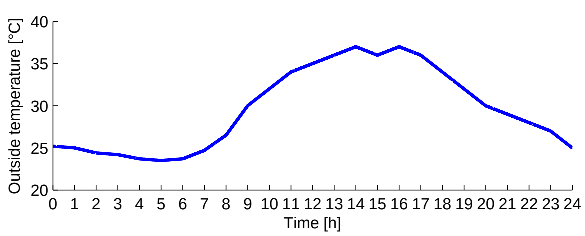


Fig. 7. Outside ambient temperature.

*3) Chiller plant optimization:* Fig. 8 shows the COP of the chiller plant as a function of the requested cooling power $Q_C$ and of the outside ambient temperature $T_a$ for $T_{pipe} = T_{pipe}^\circ = 15°C$, when the designed commitment parameters $\alpha_i^\star$ are adopted. Both chillers provide a maximum cooling power supply $Q_{c,i}^{max}$ of 30 kW, but with quite different efficiency curves. In particular, chiller 1 performs better for low power values, whereas chiller 2 prevails at higher powers. This results in a complex optimal commitment policy.

*4) ADP solution:* The policy that modulates the zone temperature set point and the chillers cooling power request is a look-up table function of:

- The discrete time $k$ at which the policy is applied, which corresponds to the interval $[\tau_k, \tau_{k+1})$
- The zone temperature $\hat{T}_z$ at $\tau_k$
- The number of occupants $\hat{n}_P$ at $\tau_k$
- The level of cold water in the storage $\hat{h}_c$ at $\tau_k$
- The value of the discomfort variable $\hat{d}$ at $\tau_k$

and is obtained with the designed commitment parameters for the two chillers in place.

We now try to get some insight into the strategy implemented by the computed policy by looking at its behavior on the nominal occupancy profile. Relevant quantities are drawn in Fig. 9 with

TABLE I
List of System Parameters

| | | |
|---|---|---|
| Zone | $C_z$ | $6092\ kJ\,°C^{-1}$ |
| | $k_{out}$ | $0.4625\ kW\,°C^{-1}$ |
| $T_z$ controller | $k_p^z$ | $9.25\ °C^{-1}$ |
| | $k_{i,z}$ | $0.075\ °C^{-1}\,s^{-1}$ |
| | $T_z^\circ$ | $20°C$ |
| Thermal storage | $C_{st}$ | $2.22 \cdot 10^4\ kJ\,°C^{-1}$ |
| | $h_{st}$ | $3\ m$ |
| | $\delta h_{st}$ | $0.03\ m$ |
| CHWC | $C_{ch}$ | $1.31 \cdot 10^3\ kJ\,°C^{-1}$ |
| | $C_{pipe}$ | $1.31 \cdot 10^3\ kJ\,°C^{-1}$ |
| | $k_{cw}$ | $5.29\ kW\,°C^{-1}$ |
| $T_{pipe}$ controller | $k_p^{pipe}$ | $14.4\ kg\,s^{-1}\,°C^{-1}$ |
| | $k_i^{pipe}$ | $0.6\ kg\,s^{-2}\,°C^{-1}$ |
| | $T_{pipe}^\circ$ | $15\ °C$ |
| $T_{ch}$ controller | $k_p^{ch}$ | $200\ kW\,°C^{-1}$ |
| | $k_i^{ch}$ | $1\ kW\,s^{-1}\,°C^{-1}$ |
| | $k_p^{w_{ch}}$ | $14.4\ kg\,s^{-1}\,°C^{-1}$ |
| | $T_{ch}^\circ$ | $10\ °C$ |
| Chiller 1 | $a_{1,1}$ | $0.0056\ kW\,K^{-1}$ |
| | $a_{1,2}$ | $10.11\ kW$ |
| | $a_{1,3}$ | $7\ K\,kW^{-1}$ |
| | $a_{1,4}$ | $0.9327$ |
| | $Q_{c,1}^{max}$ | $30\ kW$ |
| Chiller 2 | $a_{2,1}$ | $0.0109\ kW\,K^{-1}$ |
| | $a_{2,2}$ | $20.22\ kW$ |
| | $a_{2,3}$ | $3.807\ K\,kW^{-1}$ |
| | $a_{2,4}$ | $0.9325$ |
| | $Q_{c,2}^{max}$ | $30\ kW$ |
| Internal heat gain | $a_1$ | $-0.2199\ W\,°C^{-2}$ |
| | $a_2$ | $5.0597\ W\,°C^{-1}$ |
| | $a_3$ | $84.9168\ W$ |

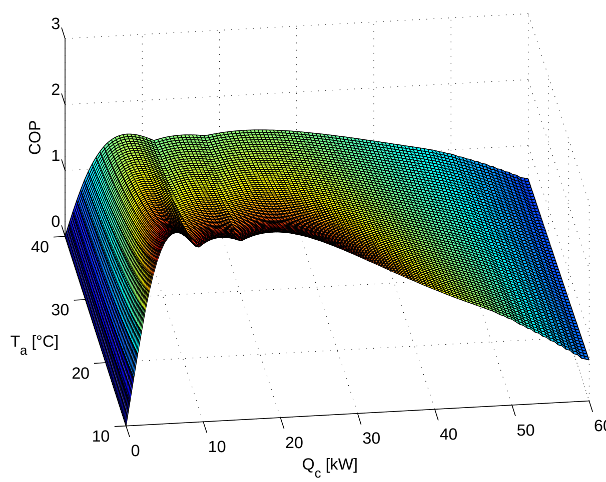


Fig. 8. COP of the chiller plant obtained via the optimization procedure in Section IV.

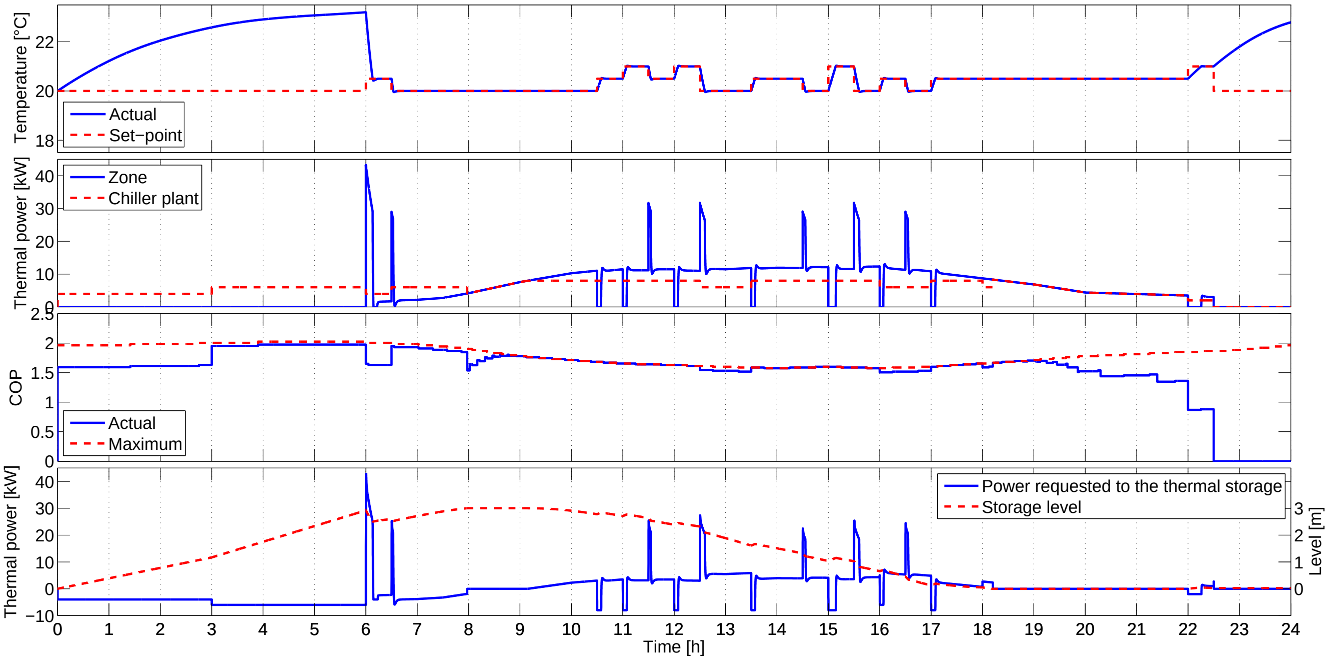


Fig. 9. Performance of the designed energy management system in the nominal occupancy case. From top to bottom: Zone temperature (blue solid line) and set-point modulation (red dashed line); Cooling power absorbed by the zone (blue solid line) and requested to the chiller plant (red dashed line); Actual (blue solid line) and maximum chiller plant COP; Cooling power request to the thermal storage (blue solid line, left axis) and level of the cold water in the storage tank (red dashed line, right axis).

reference to the whole 24 hours horizon.

In the top plot of Fig. 9, the zone temperature set-point is reported together with the actual temperature behavior. Given that the zone is cooled only from 6:00 to 22:30, its temperature tracks well the set point within that time interval, whereas it is uncontrolled outside. Notice that most of the temperature set-point modulation occurs between 10:30 and 15:30, where the occupancy profile displays its peaks, in order to reduce the cooling power demand. A further set-point modulation appears to be convenient when the storage is exhausted (at 22:00). Indeed, compared to previous time steps, the outside temperature is lower, leading to a slower transient of the zone temperature, which in turn keeps the chiller plant inactive for a longer period.

The chiller power request profile is shown in the second plot from the top of Fig. 9, together with the cooling power absorbed by the zone. Notice that the chiller power request follows the cooling load demand when the storage is not available because it is either full or empty (see the bottom plot of Fig. 9 where the level of cold water in the storage tank is shown). On the other hand, when the storage is available, the chiller power request does not have to supply the whole load demand, and it can be set equal to a value that makes it operate at the highest efficiency. This is actually shown in the third plot from the top in the same figure, where the COP of the chiller plant is very close to the maximal achievable COP for most of the time. In those time slots when the COP is not maximal, like at the start of the day till 3:00, the cooling power request to the chiller is lower so that the electric power consumption is still small.

The possibility of operating the chiller plant at its highest efficiency level is granted by the thermal storage. The bottom plot in Fig. 9 refers to the thermal storage usage by the computed policy. Charging takes place essentially in the early hours of the day, when the building is empty, but, interestingly enough, after a brief discharge transient coincident with the activation of the cooling phase, the storage unit is further charged to its maximum level to be used afterwards. Indeed, the thermal storage compensates for power mismatches, given that the chiller plant is driven on purpose at a constant power level for better efficiency, and is effective in this task for most of the day and especially in the peak hours. When the storage is exhausted the power request to the chiller plant cannot be kept constant anymore and follows the actual request.

To better understand the dynamics enforced by the energy management system, a detail of Fig. 9 is shown in Fig. 10. The temperature set-point modulation triggers a nearly instantaneous variation in the power absorbed by the zone, which is essentially provided by the thermal storage. This action is very rapid since it is enacted by regulating the cold water flow. Nevertheless it takes some time to reach the new temperature set-point, due to the thermal inertia of the zone. When this occurs the water flow is returned to the original level, and after a short and negligible transient, the temperature reaches a steady state.

For comparative purposes, we consider also the case when there is no thermal storage and no temperature set-point modulation. In this configuration, the cooling power requested to the chiller cannot be set constant to operate it at the best efficiency level since the chiller is the only source of cooling power and has to supply the cooling power requested by the zone. As a consequence it follows the profile in Fig. 11, characterized by a large amount of cooling power request at the onset of the cooling period to bring the zone temperature at its set-point.

Plots of the electrical power and energy consumption of the chillers for the two mentioned cases are reported in Fig. 12. In the absence of storage and temperature set-point modulation the chillers are forced to follow the load request, thus often operating at non-optimal efficiency. This results in an overall increased electrical energy consumption, as expected.

The value function associated to the DP equations is a good indicator of the control system performance in terms of energy saving, in that it provides (an estimate of) the expected value of the energy consumption with respect to the stochasticity in the occupancy profile. The obtained values are reported in Table II. A 21% gain is achieved with respect to a reference policy where only the chiller commitment is optimized, while the temperature set-point is set constant to 20°C and the thermal storage is not available (so that the chillers must always supply the exact amount of requested cooling power). The

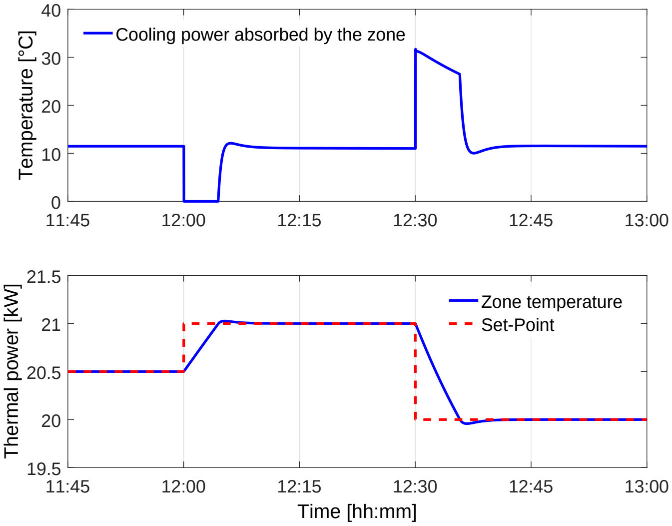


Fig. 10. Detail of Fig. 9. From top to bottom: Cooling power absorbed by the zone; Zone temperature (blue solid line) and optimal set-point modulation (red dashed line).

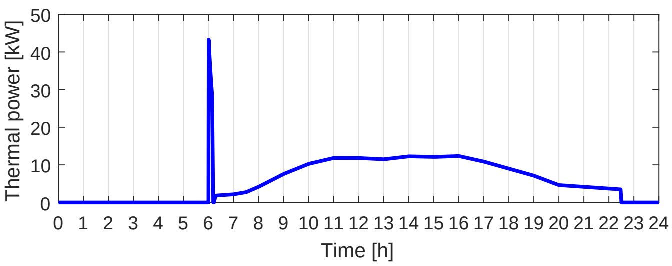


Fig. 11. Power flows in the system in the absence of thermal storage and set-point modulation: the cooling power requested to the chiller plant has to match that absorbed by the zone.

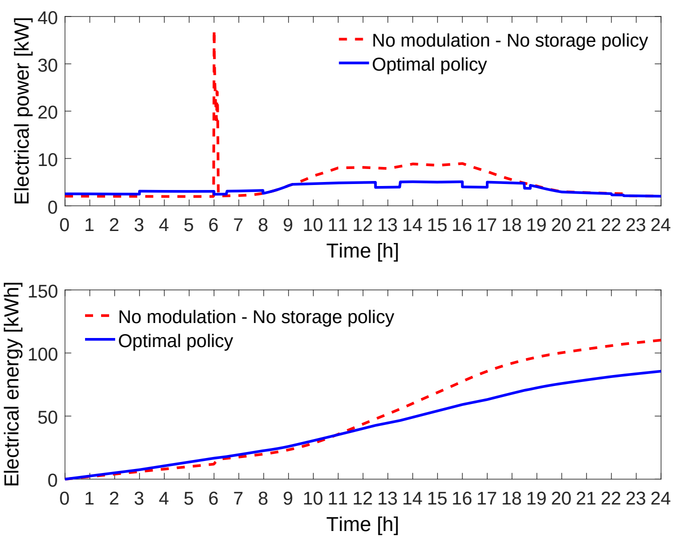


Fig. 12. Electrical power (top) and energy (bottom) consumption: designed policy (solid blue) and results in the absence of storage and temperature set-point modulation (dashed red).

thermal storage is mostly to be credited for the obtained benefit, since the temperature modulation alone can only save 2.5 kWh. Indeed, thanks to the storage the chiller plant can be employed at highly efficient operation regimes.

TABLE II
VALUE FUNCTION FOR THE OPTIMAL POLICY IN DIFFERENT CONDITIONS.

| Thermal storage | Set-point modulation | Value function |
|---|---|---|
| no | no | 107.83 $kWh$ |
| no | yes | 105.43 $kWh$ |
| yes | no | 87.86 $kWh$ |
| yes | yes | 85.19 $kWh$ |

## A. Comparative analysis

In this section, we compare the optimal policy performance against that obtained with a "smart" heuristic policy. In the heuristic policy, all the allowed zone temperature set-point modulation is used in the range of consecutive hours where the occupancy is larger (i.e., from 10:30 to 16:30). As for the chillers cooling power request, it is set constant and equal to 8 kW (which approximately corresponds to the highest COP value) from 00:00 to 17:00, while from 17:00 to 24:00 it is set to zero so as to empty the storage at the very end of the day when the minimum occupancy profile occurs. With this choice, at the end of the day the storage will be empty for every occupancy profile, as it is the case for the optimal policy which minimizes the electrical energy consumption over the one-day finite horizon.

In order to provide statistical evidence of the efficacy of our approach, we run $M$ = 5128 Monte Carlo simulations of the electric energy consumption where both the optimal policy and the heuristic policy are applied to the same occupancy profiles, extracted independently according to the probabilistic model in Section II-C. The number $M$ of simulations is set according to Hoeffding's inequality so as to obtain an accuracy $\varepsilon$ = 1 kWh with confidence larger than of equal to $1-\delta = 0.99$ in the estimation of the average electric energy consumption.

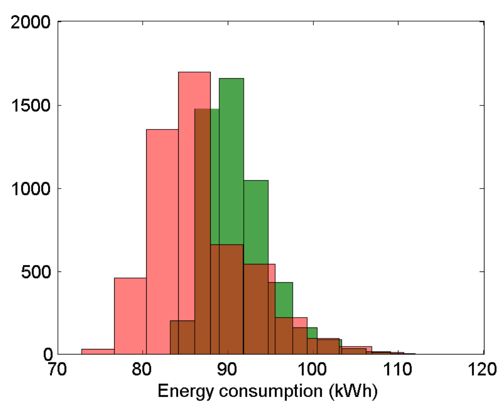


Fig. 13. Histograms of the electric energy consumption obtained with $M = 5128$ simulations: optimal policy (red) and heuristic policy (green).

The resulting histograms are plotted in Fig. 13 and clearly show that the optimal policy has a better performance since its histogram is shifted to lower values than that of the heuristic policy. This is further witnessed by the empirical mean value, which is equal to 86.57 kWh for the optimal policy and 91.04 kWh for the heuristic policy. As a side remark, note also that the empirical mean obtained for the optimal policy is very close to the value 85.19 kWh reported in Table II for the same configuration, although it differs more than the value set for the accuracy $\varepsilon = 1$ kWh. This is not surprising since the value function is computed based on an approximate quantized model with the state re-initialized to a quantized value on the grid every $\tau$ minutes, and, as such it is only an estimate of the mean.

Fig. 14 represents the same plots of Fig. 9 for the heuristic policy applied to the nominal occupancy profile. The electric energy

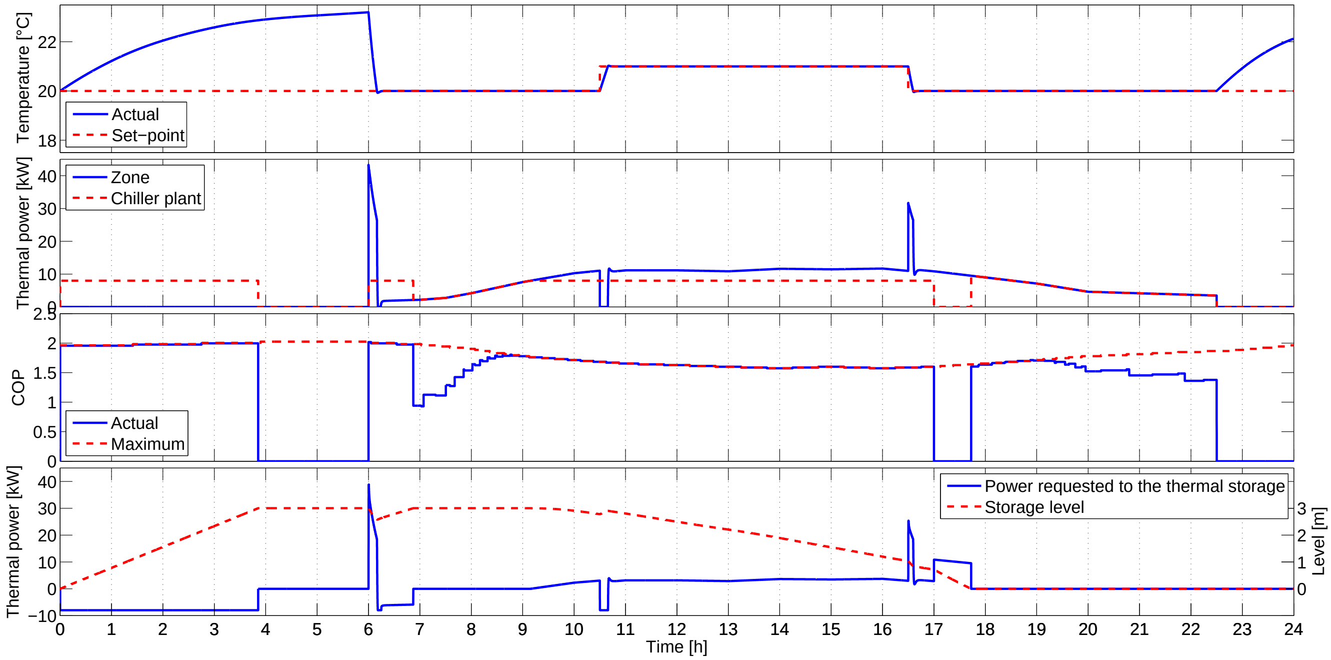


Fig. 14. Performance of the heuristic policy in the nominal occupancy case. From top to bottom: Zone temperature (blue solid line) and set-point modulation (red dashed line); Cooling power absorbed by the zone (blue solid line) and requested to the chiller plant (red dashed line); Actual (blue solid line) and maximum chiller plant COP; Cooling power request to the thermal storage (blue solid line, left axis) and level of the cold water in the storage tank (red dashed line, right axis).

consumption in this case is 90.32 kWh while it is 85.55 kWh when the optimal policy is applied.

## VIII. Conclusions and Future Work

In this paper, we have considered the optimal energy management of a building cooling system with thermal storage and addressed its solution through a procedure that was suggested in [2] with reference to a deterministic simpler setting with no storage unit. The procedure is based on the integration of nonlinear static optimization into dynamic programming and requires the abstraction of the stochastic hybrid system under consideration to a controlled Markov chain for the actual computation of the policy in a tabular, easy to implement, form. A parallel implementation of the approximate dynamic programming solution through GPU-accelerated computing has been adopted to speed up the policy calculation.

The proposed framework is currently extended to the case of a micro-grid that includes further components, such as local electric power consumption due to electric appliances and generation from renewable energy sources or via co-generation units. The presence of these additional elements offers additional flexibility to the energy management system, but also makes the energy management task more difficult to solve because of the growth of the state space dimension and the further stochastic elements.

## References


[1] J. Gordon, K. Ng, and H. Chua, "Optimizing chiller operation based on finite-time thermodynamics: universal modeling and experimental confirmation," *International Journal of Refrigeration*, vol. 20, no. 3, pp. 191–200, 1997.

[2] N. Ceriani, R. Vignali, L. Piroddi, and M. Prandini, "An approximate dynamic programming approach to the energy management of a building cooling system," in *European Control Conference*, Zurich, Switzerland, July 17-19 2013, pp. 2026–2031.

[3] A. Girard and G. Pappas, "Approximate bisimulation: A bridge between computer science and control theory." *European Journal of Control*, vol. 17, no. 5-6, pp. 568–578, 2011.

[4] A. Julius, A. Girard, and G. Pappas, "Approximate bisimulation for a class of stochastic hybrid systems," in *Proceedings of the American Control Conference*, Minneapolis (MA), USA, June 14-16 2006.

[5] A. Julius and G. Pappas, "Approximate abstraction of stochastic hybrid systems," *IEEE Transactions on Automatic Control*, vol. 54, no. 6, pp. 1193–1203, 2009.

[6] A. Abate and M. Prandini, "Approximate abstractions of stochastic systems: a randomized method," in $50^{th}$ *IEEE Conference on Decision and Control and European Control Conference (CDC-ECC)*, Orlando (FL), USA, Dec. 12-15 2011, pp. 4861–4866.

[7] S. Garatti and M. Prandini, "A simulation-based approach to the approximation of stochastic hybrid systems," in *$4^{th}$ IFAC Conference on Analysis and Design of Hybrid Systems (ADHS'12)*, Eindhoven, The Netherlands, June 4-8 2012, pp. 1108–1113.

[8] M. Prandini, S. Garatti, and R. Vignali, "Performance assessment and design of abstracted models for stochastic hybrid systems through a randomized approach," *Automatica*, vol. 50, no. 11, pp. 2852 – 2860, 2014. [Online]. Available: http://www.sciencedirect.com/science/article/pii/S0005109814003458

[9] F. Oldewurtel, A. Parisio, C. Jones, D. Gyalistras, M. Gwerder, V. Stauch, B. Lehmann, and M. Morari, "Use of model predictive control and weather forecasts for energy efficient building climate control," *Energy and Buildings*, vol. 45, pp. 15–27, 2012.

[10] Y. Ma, A. Kelman, A. Daly, and F. Borrelli, "Predictive control for energy efficient buildings with thermal storage: Modeling, stimulation, and experiments," *IEEE Control Systems Magazine*, vol. 32, no. 1, pp. 44–64, Feb. 2012.

[11] D. Ioli, A. Falsone, and M. Prandini, "Optimal energy management of a building cooling system with thermal storage: A convex formulation," in *ADCHEM*, Whistler, British Columbia, Canada, June 2015.

[12] ——, "Energy management of a building cooling system with thermal storage: a randomized solution with feedforward disturbance compensation," in *2016 American Control Conference (ACC)*, 2016, pp. 2346–2351.

[13] Y. Ma, F. Borrelli, B. Hencey, A. Packard, and S. Bortoff, "Model predictive control of thermal energy storage in building cooling systems," in *Proceedings of the* $48^{th}$ *IEEE Conference on Decision and Control /* $28^{th}$ *Chinese Control Conference*, Shanghai, P.R. China, Dec. 16-18 2009, pp. 392–397.

[14] Y. Ma, F. Borrelli, B. Hencey, B. Coffey, S. Bengea, and P. Haves, "Model predictive control for the operation of building cooling systems,"

in *American Control Conference*, Baltimore (MD), USA, June 30 - July 2) year = 2010, pp. 5106–5111.

[15] M. Behl, T. Nghiem, and R. Mangharam, “Green scheduling for energy-efficient operation of multiple chiller plants,” in *33rd IEEE Real-Time Systems Symposium (RTSS)*, San Juan, Puerto Rico, Dec. 4-7 2012, pp. 195–204.

[16] A. Parisio, E. Rikos, and L. Glielmo, “A model predictive control approach to microgrid operation optimization,” *IEEE Transactions on Control Systems Technology*, vol. 22, no. 5, pp. 1813–1827, Sept 2014.

[17] A. Parisio, E. Rikos, G. Tzamalis, and L. Glielmo, “Use of model predictive control for experimental microgrid optimization,” *Applied Energy*, vol. 115, pp. 37–46, 2014.

[18] K. Deng, Y. Sun, S. Li, Y. Lu, J. Brouwer, P. G. Mehta, M. C. Zhou, and A. Chakraborty, “Model predictive control of central chiller plant with thermal energy storage via dynamic programming and mixed-integer linear programming,” *IEEE Transactions on Automation Science and Engineering*, vol. 12, no. 2, pp. 565–579, April 2015.

[19] V. Putta, D. Kim, J. Cai, J. Hu, and J. Braun, “Model predictive controllers for the joint optimization of zone dynamics and equipment operation in multi-zone buildings: A case study,” in *Intelligent Building Workshop*, 2013.

[20] V. Putta, G. Zhu, D. Kim, J. Hu, and J. Braun, “A distributed approach to efficient model predictive control of building HVAC systems,” in *2nd Int. High Performance Buildings Conference*, 2012.

[21] V. Putta, D. Kim, J. Cai, J. Hu, and J. Braun, “Distributed model predictive control for building HVAC systems: A case study,” in *3rd Int. High Performance Building Conf. at Purdue*, July 14-17 2014.

[22] X. Zhang, G. Schildbach, D. Sturzenegger, and M. Morari, “Scenario-Based MPC for Energy-Efficient Building Climate Control under Weather and Occupancy Uncertainty,” in *European Control Conference*, Zurich, Switzerland, Jul. 2013, pp. 1029–1034. [Online]. Available: http://control.ee.ethz.ch/index.cgi?page=publications;action=details;id=4464

[23] F. Oldewurtel, C. Jones, A. Parisio, and M. Morari, “Stochastic model predictive control for building climate control,” *IEEE Transactions on Control Systems Technology*, vol. 22, no. 3, pp. 1198–1205, 2014.

[24] A. Abate, M. Prandini, J. Lygeros, and S. Sastry, “Probabilistic reachability and safety for controlled discrete time stochastic hybrid systems,” *Automatica*, vol. 44, no. 11, pp. 2724 – 2734, 2008.

[25] S. Summers and J. Lygeros, “Verification of discrete time stochastic hybrid systems: A stochastic reach-avoid decision problem,” *Automatica*, vol. 46, no. 12, pp. 1951 – 1961, 2010.

[26] D. P. Bertsekas, *Dynamic Programming and Optimal Control, Vol. II: Approximate Dynamic Programming*. Athena Scientific, 2012.

[27] F. Borghesan, R. Vignali, L. Piroddi, M. Strelec, and M. Prandini, “Micro-grid energy management: a computational approach based on simulation and approximate discrete abstraction,” in *52nd IEEE Conference on Decision and Control*, Firenze, Italy, December 10-13 2013.

[28] F. Borghesan, R. Vignali, L. Piroddi, M. Prandini, and M. Strelec, “Approximate dynamic programming-based control of a building cooling system with thermal storage,” in *4th European Innovative Smart Grid Technologies (ISGT) Conference*, Copenhagen, Denmark, October 6-9 2013.

[29] D. Kim and J. E. Braun, “Reduced-order building modeling for application to model-based predictive control,” in *5th National Conference of IBPSA-USA*, Madison, Wisconsin, USA, August 1–3 2012, pp. 554–561.

[30] D. Kim, W. Zuo, J. E. Braun, and M. Wetter, “Comparisons of building system modeling approaches for control system design,” in *13th Conference of International Building Performance Simulation Association*, Chambery, France, August 26–28 2013, pp. 3267–3274.

[31] D. Ioli, A. Falsone, S. Schuler, and M. Prandini, “A compositional framework for energy management of a smart grid: A scalable stochastic hybrid model for cooling of a district network,” in *2016 12th IEEE International Conference on Control and Automation (ICCA)*, June 2016, pp. 389–394.

[32] P. Sreedharan and P. Haves, “Comparison of chiller models for use in model-based fault detection,” in *Int. Conf. for Enhanced Building Operations (ICEBO)*, Austin (TX), USA, July 16-19 2001.

[33] I. Dinçer and M. A. Rosen, *Thermal energy storage: systems and applications*. Chichester, UK: John Wiley & Sons, Ltd, 2001.

[34] *CIBSE Guide A: Environmental Design*. Norwich, UK: CIBSE Publications, 2006.

[35] J. Page, D. Robinson, N. Morel, and J.-L. Scartezzini, “A generalised stochastic model for the simulation of occupant presence,” *Energy and Buildings*, vol. 40, no. 2, pp. 83–98, 2008.

[36] M. Campi, S. Garatti, and M. Prandini, “The scenario approach for systems and control design,” *Annual Reviews in Control*, vol. 33, no. 2, pp. 149–157, 2009.

## Appendix: Proof of Proposition 1

Note that $\alpha_i^\star[Q_c]$ can be expressed as:

$$\alpha_i^\star[Q_c] = (1-\alpha_n^\star[Q_c])\theta_i[Q_c] \tag{25}$$

where $0 \leq \theta_i[Q_c] \leq \min\{Q_{c,i}^{\max}/Q_c, 1\}$, $i = 1,\dots,n-1$, and $\sum_{i=1}^{n-1}\theta_i[Q_c] = 1$. We next show that

$$\theta_i[Q_c] = \beta_i^\star[(1-\alpha_n^\star[Q_c])Q_c],\ i = 1,\dots,n-1. \tag{26}$$

Indeed, by the definition of $\beta_i^\star(Q_c)$ as the optimizer for problem (11), and denoting by $P_{e,i}^\star[Q_c]$ the optimal value of $P_{e,i}$ obtained by solving (10), we have that

$$\begin{aligned}
&\sum_{i=1}^{n-1} P_{e,i}[\beta_i^\star[(1-\alpha_n^\star[Q_c])Q_c]\cdot(1-\alpha_n^\star[Q_c])Q_c] \\
&\quad\leq \sum_{i=1}^{n-1} P_{e,i}[\theta_i[Q_c]\cdot(1-\alpha_n^\star[Q_c])Q_c] \\
&\quad= \sum_{i=1}^{n-1} P_{e,i}[\alpha_i^\star[Q_c]Q_c] = \sum_{i=1}^{n-1} P_{e,i}^\star[Q_c],
\end{aligned}$$

which entails that

$$\begin{aligned}
&\sum_{i=1}^{n-1} P_{e,i}[\beta_i^\star[(1-\alpha_n^\star[Q_c])Q_c]\cdot(1-\alpha_n^\star[Q_c])Q_c] \\
&\quad+ P_{e,n}^\star[Q_c] \leq \sum_{i=1}^{n} P_{e,i}^\star[Q_c],
\end{aligned}$$

and proves (26).

Now we only need to prove (13), which implies (14) given that equations (26) and $\gamma_2^\star[Q_c] = 1-\gamma_1^\star[Q_c]$ hold.

Since $\gamma_1^\star$ and $\gamma_2^\star$ are the solution to (12), we have that

$$\begin{aligned}
&P_{e,[1,n-1]}^\star[\gamma_1^\star[Q_c]Q_c] + P_{e,n}[\gamma_2^\star[Q_c]Q_c] \\
&= P_{e,[1,n-1]}^\star[(1-\gamma_2^\star[Q_c])Q_c] + P_{e,n}[\gamma_2^\star[Q_c]Q_c] \\
&\leq P_{e,[1,n-1]}^\star[(1-\alpha_n^\star[Q_c])Q_c] + P_{e,n}[\alpha_n^\star[Q_c]Q_c].
\end{aligned}$$

Observe now that

$$\begin{aligned}
&P_{e,[1,n-1]}^\star[(1-\alpha_n^\star[Q_c])Q_c] \\
&\quad= \sum_{i=1}^{n-1} P_{e,i}[\beta_i^\star[(1-\alpha_n^\star[Q_c])Q_c]\cdot(1-\alpha_n^\star[Q_c])Q_c] \\
&\quad= \sum_{i=1}^{n-1} P_{e,i}^\star[Q_c]
\end{aligned}$$

where the first equality follows from the definition of $\beta_i^\star$ and the second one from equation (25) combined with (26). Plugging this result into the previous equation, we obtain

$$\begin{aligned}
&P_{e,[1,n-1]}^\star[(1-\gamma_2^\star[Q_c])Q_c] + P_{e,n}[\gamma_2^\star[Q_c]Q_c] \\
&\quad\leq \sum_{i=1}^{n-1} P_{e,i}^\star[Q_c] + P_{e,n}[\alpha_n^\star[Q_c]Q_c] \\
&\quad= \sum_{i=1}^{n} P_{e,i}^\star[Q_c],
\end{aligned}$$

which show that the optimal fraction of $Q_c$ to be assigned to chiller $n$ is $\alpha_n^\star[Q_c] = \gamma_2^\star[Q_c]$. This concludes the proof.